Sphingosine kinase 1 overexpression is regulated by signaling through PI3K, AKT2, and mTOR in imatinib-resistant chronic myeloid leukemia cells

Gabriella Marfe[a], Carla Di Stefano[a], Alessandra Gambacurta[a], Tiziana Ottone[b,c], Valentina Martini[a], Elisabetta Abruzzese[d], Luca Mologni[e], Paola Sinibaldi-Salimei[a], Paolo de Fabritis[f], Carlo Gambacorti-Passerini[e], Sergio Amadori[d], and Raymond B. Birge[g]

[a]Department of Experimental Medicine and Biochemical Sciences, University of Rome "Tor Vergata," Rome, Italy; [b]Department of Biopathology and Diagnostic Imaging, University "Tor Vergata," Rome, Italy; [c]Laboratory of Neuro-Onco-Hematology, Santa Lucia Foundation, Rome, Italy; [d]Department of Haematology, University of Rome "Tor Vergata," Rome, Italy; [e]Department of Clinical Medicine and Prevention, University of Milano-Bicocca, Monza, Italy; [f]Department of Haematology, S. Eugenio Hospital Rome, Rome, Italy; [g]Department of Biochemistry and Molecular Biology, University of Medicine and Dentistry of New Jersey, New Jersey Medical School, Newark, NJ., USA

(Received 28 September 2010; revised 18 February 2011; accepted 26 February 2011)

Objective. As a better understanding of the molecular basis of carcinogenesis has emerged, oncogene-specific cell-signaling pathways have been successfully targeted to treat human malignances. Despite impressive advances in oncogene-directed therapeutics, genetic instability in cancer cells often manifest acquired resistance. This is particularly noted in the use of tyrosine kinase inhibitors therapies and not more evident than for chronic myeloid leukemia. Therefore, it is of great importance to understand the molecular mechanisms affecting cancer cell sensitivity and resistance to tyrosine kinase inhibitors.

Materials and Methods. In this study, we used continuous exposure to stepwise increasing concentrations of imatinib ($0.6-1$ μM) to select imatinib-resistant K562 cells.

Results. Expression of BCR-ABL increased both at RNA and protein levels in imatinib-resistant cell lines. Furthermore, expression levels of sphingosine kinase 1 (SphK1) were increased significantly in resistant cells, channeling sphingoid bases to the SphK1 pathway and activating sphingosine-1-phosphate−dependent tyrosine phosphorylation pathways that include the adaptor protein Crk. The partial inhibition of SphK1 activity by *N,N*-dimethylsphingosine or expression by small interfering RNA increased sensitivity to imatinib-induced apoptosis in resistant cells and returned BCR-ABL to baseline levels. To determine the resistance mechanism-induced SphK1 upregulation, we used pharmacological inhibitors of the phosphoinositide 3-kinase/AKT/mammalian target of rapamycin signaling pathway and observed robust downmodulation of SphK1 expression and activity when AKT2, but not AKT1 or AKT3, was suppressed.

Conclusions. These results demonstrate that SphK1 is upregulated in imatinib-resistant K562 cells by a pathway contingent on a phosphoinositide 3-kinase/AKT2/mammalian target of rapamycin signaling pathway. We propose that SphK1 plays an important role in development of acquired resistance to imatinib in chronic myeloid leukemia cell lines.   © 2011 ISEH - Society for Hematology and Stem Cells.   Published by Elsevier Inc.

Chronic myeloid leukemia (CML) is characterized by the presence of the Philadelphia chromosome resulting from a balanced reciprocal translocation between the long arms of chromosomes 9 and 22. This exchange brings together two genes: the *Bcr* gene on chromosome 22 and the nonreceptor tyrosine kinase proto-oncogene *Abl* on chromosome 9 [1–3]. One of the major advancements in the treatment of CML has been the development of imatinib (IM), which shows striking activity in the chronic and accelerated phases, but less activity in the blast phase of the disease [4,5]. Imatinib directly associates with the adenosine triphosphate−binding site of the BCR-ABL tyrosine kinase and locks the enzyme in its inactive conformation [6].

Inhibition of BCR-ABL by IM also results in transcriptional downmodulation of various genes involved in the control of cell cycle, cell adhesion, and cytoskeleton organization leading to apoptotic cell death [7]. Development of resistance to IM includes BCR-ABL−dependent mechanisms, such as modification of the target BCR-ABL tyrosine kinase through gene amplification/mutation, or independent mechanisms that involve epigenetic changes in the expression of survival factors [8–12].

Among the survival pathways activated by BCR-ABL, the phosphoinositide 3-kinase (PI3K)/AKT/mammalian target of rapamycin (mTOR) pathway is constitutively active in CML cells and plays a major role in cell survival [12,13]. Furthermore, a recent study has emphasized the importance of dysregulated translation in a wide range of human malignancies and has also emphasized the important role of mTOR and its effectors in oncogenesis [14–16]. Hence, it is plausible that dysregulated translation is also important in the pathogenesis of BCR-ABL−positive leukemia.

In the present study, we used a genetic selection strategy to generate IM-resistant K562 (K562 IM/R), and unexpectedly found that IM/R cells displayed significantly increased sphingosine kinase 1 (SphK1) expression and activity. SphK1 plays a pivotal role in sphingosine metabolism, catalyzing the phosphorylation of sphingosine to sphingosine 1-phosphate (S1P), a potent intracellular and extracellular messenger. SIP binds to S1P receptor, a G-protein−coupled receptor, stimulating growth and survival pathways. In particular, increased intracellular levels of SphK1 contribute to cell growth, survival, and transformation in leukemia models [17–23]. S1P has been shown to activate several signal transduction pathways, including those that implicated in tyrosine phosphorylation, such as the tyrosine phosphorylation of the Crk adaptor protein [24,25].

We also show here that SphK1 is critical for maintaining the IM/R phenotype in K562 cells as small interfering RNA (siRNA) and pharmacological inhibitors of SphK1 decrease BCR-ABL expression and restore the sensitivity of these cells to IM. Furthermore, using a panel of pharmacological inhibitors, we show that the PI3K/AKT/mTOR pathway modulates SphK1 expression and is required to stabilize SphK1 expression levels. Drug-resistance−stimulated increases in SphK1 messenger RNA (mRNA), protein, and enzymatic activity levels were significantly reduced in cells that had been transfected with AKT2 siRNA, but not AKT1 or AKT3 siRNA, suggesting that AKT2 is critical for regulation of SphK1 expression in resistant CML cells.

This study identifies a role for the ceramide/S1P pathway in the mechanisms of resistance to IM in K562 cells and suggests that acquired drug resistance to tyrosine kinase inhibitors (TKIs) in human cancer cells is accompanied by activation of SphK1 and by establishment of an amplification loop that drives cell proliferation and survival. Furthermore, these data demonstrate that the PI3K/AKT/mTOR signaling pathway is involved in regulation of SphK1, with AKT2 playing a key role in drug-resistance−induced SphK1 expression in K562 IM/R cells.

Materials and methods

Cells and culture conditions
K562 cell line was grown in RPMI-1640 medium (Gibco, Frederick, MD, USA). Resistant clones K562 IM/R have been established by continuous exposure to IM [7,26]. To produce IM/R cells, we incubated K562 cells with either 0.6 μM or 1.0 μM IM for 3 weeks, and both procedures gave identical results. Here, we only show the results of the 0.6 μM IM/R cells.

Materials
Imatinib and everolimus (1 nM) was supplied by Novartis (Switzerland, Basel). Wortmannin (100 nM; Biomol, Plymouth Meeting, PA, USA), SH-5 (5 μM; Alexis Biochemicals, San Diego, CA, USA) and N,N-dimethylsphingosine (DMS) were prepared in dimethyl sulfoxide. 4-Amino-5-(4-chlorophenyl)-7-(t-butyl)pyrazolo[3,4-d]pyrimidine and 2′-amino-3′-methoxyflavone (PD98059) were purchased from Calbiochem (New York, NY, USA).

Molecular analysis
With the aim of analyzing ABL mutations, we used strategy based on a direct sequencing as reported previously [27].

RNA isolation and complementary DNA preparation
Total RNA was isolated from samples using Trizol reagent (Gibco; Invitrogen, Frederick, MD, USA). RNA was reverse-transcribed using a random hexanucleotide primer with Superscript II Reverse Transcriptase according to manufacturer's instructions (Invitrogen).

Semi-quantitative reverse transcription polymerase chain reaction analysis
Primer pairs sequences were BCR exon 2: 5-GGAGCTGCAGATGC TGACCACC-3, ABL: 5-TCAGACCCTGAGGCTCAAAGTC-3. The primers for the human β-actin gene were: 5-AGCGGGAA ATCGTGCGTGACA-3, 5-GTGGACTTGGGAGAGGACTGG-3 (Epicentre Biotechnologies, Madison, WI, USA).

Southern blot analysis
The DNA samples were separated on agarose gel and transferred onto a nylon membrane. Hybridization was carried as described previously [28].

Reverse transcription polymerase chain reaction
The sequences of the primers and probe used for BCR-ABL have been described previously [29].

Apoptosis assay
Apoptosis was quantified using the Annexin V−fluorescein isothiocyanate apoptosis kit (BD Biosciences, Franklin Lakes, NJ, USA) in accordance with manufacturer's instructions.

Transfection of human SphK1 in human cell lines
Human SphK1 (GenBank accession no. AF200328) complementary DNA was cloned into pCMV6-AC-GFP (OriGene, Rockville, MD USA). Stable transfections were performed using the LipofectAMINE 2000 (Invitrogen) according to manufacturer's protocols.

Hairpin siRNA construct for Sphk1, AKT1, AKT2, AKT3, Erk1/2, and c-Src

Endogenous Sphk1 expression was downregulated with sequence-specific p*Silencer*-siSphK1 851 (Clone1) and 1118 (Clone2) as described previously [30]. Endogenous AKT1, AKT2, and AKT3 expression was downregulated by siRNA for AKT1, AKT2, or AKT3 (Dharamcon, Lafayette, CO, USA).

Hairpin siRNA construct for Erk1/2 and c-Src RNA interference experiments were performed with siRNA for Erk1, Erk2, and c-Src (Santa Cruz Biotechnology, Santa Cruz, CA, USA) using Lipofectamine 2000 reagent (Invitrogen) according to manufacturer's instructions.

Northern blot analysis

Aliquots of RNA were electrophoresed and subsequently blotted onto nylon membranes. Hybridization signals were detected with a PhosphorImager (Bio-Rad, Hercules, CA, USA). The relative amount of mRNA level was quantified using a Gel-Doc phosphorimager and Quantity One software (Bio-Rad) and normalized by the intensity of β-actin.

Protein extraction and Western blot analysis

The protein extracts, obtained from cell lysates, were electrophoresed on sodium dodecyl sulfate polyacrylamide gels and probed with the following primary antibodies: rabbit polyclonal SphK1 (Santa Cruz), rabbit polyclonal Crk (Cell Signaling Technnology, Danvers, MA, USA), rabbit polyclonal phospho-Crk (Tyr221; Cell Signaling), phospho-Crk (Tyr251), phospho-Crk (Tyr239) (Birge, unpublished data), rabbit polyclonal c-ABL (K-12), rabbit polyclonal AKT1, rabbit polyclonal AKT2, mouse polyclonal AKT3, rabbit polyclonal Erk1/2, rabbit polyclonal c-Src, mouse monoclonal caspase-3, mouse monoclonal poly(ADP-ribose) polymerase (all antibodies were purchased from Santa Cruz Biotechnology, Santa Cruz, CA, USA), rabbit polyclonal phospho-AKT (Cell Signaling), rabbit polyclonal phospho-protein kinase C (PKC) (pan) (Cell Signaling) and rabbit polyclonal β–actin antibodies (Sigma, St Louis, MO, USA). Immunoreactive proteins were visualized by enhanced chemiluminescence system (Amersham Life Science, Arlington Hts, UK). The relative amount of protein expression was quantified using a Gel-Doc phosphorimager and Quantity One software (Bio-Rad) and normalized by the intensity of β-actin.

SphK1 activity assay

The SphK1 activity assay was performed as described by Olivera et al. [18] with minor modifications. Briefly, 50 μM D-erythro-sphingosine (Avanti Polar Lipids, Alabaster, AL, USA) was combined with 200 μM ATP containing 2 μCi [γ^{32}P] ATP (ICN Radiochemicals, Costa Mesa, CA, USA) in 100 μL final volume of SphK1 Activity Assay Buffer (50 mM HEPES, 50 mM MgCl$_2$, 10 mM KCl, 10 mM NaF, 2 mM NaVO$_3$, 500 μM 4-deoxypyridoxine, 0.05% Triton X-100 [pH 7.4]). The reaction was initiated by addition of enzyme. The reaction was agitated for 20 minutes at 37°C and reactions were terminated by the addition of 10 μL 6N HCl. Labeled lipids were extracted by the addition of 250 μL chloroform:methanol:HCl (100:200:1 v/v/v, 125 μL chloroform, and 125 μL 1 M KCl). The organic phase, which contained radiolabeled S1P, was removed and scintillation counted.

Statistical analysis

Each experiment was performed at least three times, and representative data are shown. Data in bar graph are given as the mean ± standard error of mean. Means were checked for statistical difference using the *t*-test and *p* values <0.05 were considered significant (*$p < 0.05$; **$p < 0.01$; ***$p < 0.001$).

Results

Establishment of the K562 IM-resistant cell line by drug selection

Several mechanisms exist, including amplification, increased expression of the BCR-ABL protein, and point mutations in the ABL kinase domain that can mediate acquired clinical resistance to IM. In this study, to generate IM-resistant CML cells, we step-wise cultured K562 cells under IM selection (0.6 μM) for 3 weeks, and subsequently increased selection to 1.0 μM for an additional 3 weeks (Fig. 1A) [31]. After selection with a single course of 0.6 μM, we observed that resistant clones expressed higher levels of both the BCR-ABL mRNA and oncoprotein compared to parental K562 cells, as shown by Southern blot analysis of polymerase chain reaction (PCR) and Western blot (Fig. 1B−E, respectively; *p* < 0.01). To rule out the possibility that selection may have caused mutations on the kinase domain, the ABL kinase domain was sequenced after nested PCR of each of cell line and confirmed to contain no point mutations of the ABL kinase domain in the any surviving clones (data not shown).

K562 IM/R cells are more resistant to apoptosis via upregulation of SphK1

To investigate whether K562 IM/R cells with BCR-ABL levels manifested a survival advantage and suppression of apoptosis, we assessed apoptosis after exposure to imanitib. Cell death was measured by flow cytometry analysis with Annexin V−fluorescein isothiocyanate and propidium iodide staining. Consistent with the expression data, IM induced apoptosis more efficiently in K562 cells than in K562 IM/R cells (Fig. 2A, B). Several studies have shown that SphK1 overexpression contributes to acquisition of multidrug resistance [20,32–36], which remains a hurdle in the treatment of hematological malignancies, including in the context of targeted therapies. As shown in Figure 3A and B, the levels of SphK1 transcripts and protein expression were significantly higher in K562 IM/R 0.6 μM cells compared with sensitive K562 cells. Because SphK1 protein expression is not a reliable indicator of enzymatic activity, we also observed that SphK1 activity levels were significantly increased in K562 IM/R 0.6 μM compared to K562 cells (Fig. 3C). To directly assess the role of SphK1 in resistance induced by TKIs in K562 IM/R cell lines, we employed either a chemical inhibitor of SphK1 called DMS (a drug that blocks production of sphingosine-1-phosphate in the ceramide synthesis pathway) and silenced SphK1 by transfecting siRNA, or transfected SphK1 complementary DNA in sensitive K562 cells (K562-SphK1). As expected, the transfection
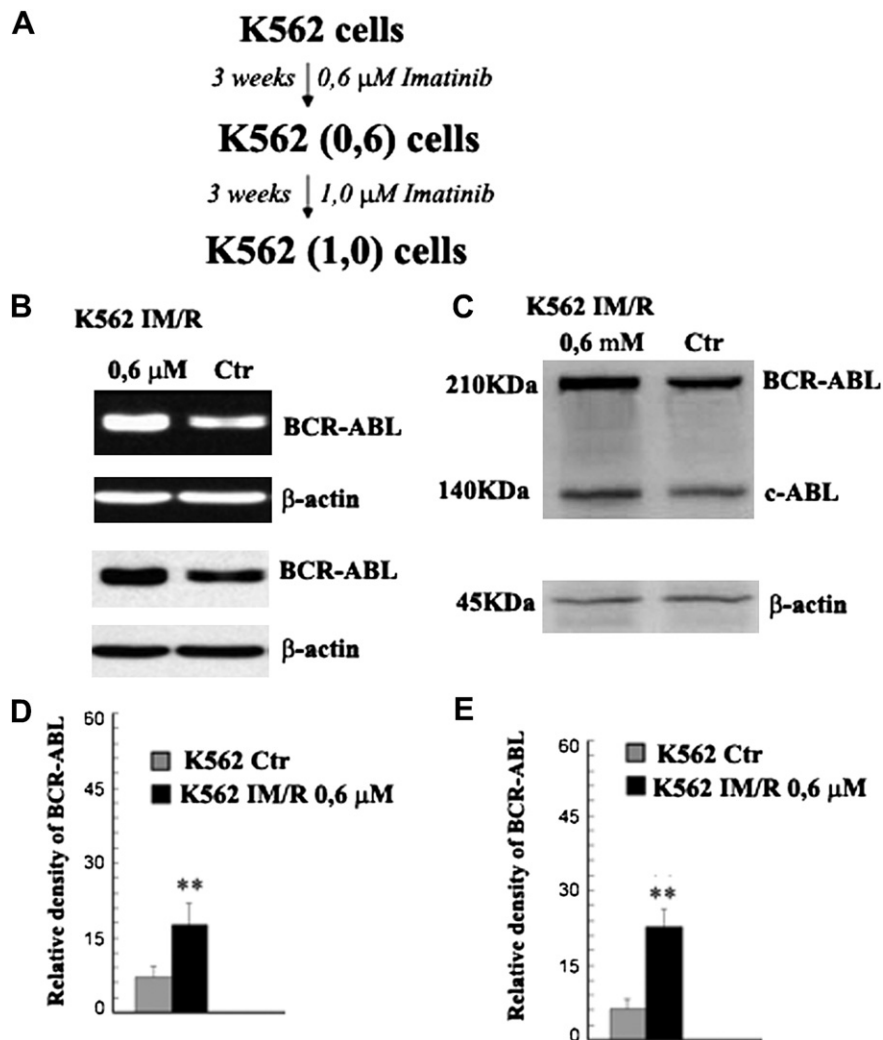
Figure 1. Selection of imatinib-resistance K562 cells. (**A**) Schematic diagram showing the selection strategy employed to generate IM/R cells. As indicated, the K562 cells were cultured under nonlethal conditions with a step-wise increased in IM (3 weeks in 0.6–1 μM IM). After selection, cells were maintained at the indicated concentrations and then analyzed for BCR-ABL complementary DNA (reverse transcription PCR: agarose gel) and Southern blot analysis (**B**) and protein (**C**). In (**C**), total lysates were immunoblotted with anti-ABL antibodies. β-actin was used as an internal loading control. The molecular weight (in KDa) of protein size standards is shown on the left-hand side. Blot is representative of three separate experiments. (**D**) Densitometric analysis of Northern blot relative to BCR-ABL. Bars represent the mean ± standard error of mean (SEM) of the results from three separate experiments. Significant differences between IM-resistant cells and control cells are indicated by probability p values. *$p < 0.05$; **$p < 0.01$; and ***$p < 0.001$. (**E**) Densitometric analysis of Western blots relative to BCR-ABL. Bars represent mean ± SEM of the results from three separate experiments. Significant differences between IM-resistant cells and control cells are indicated by probability p values. *$p < 0.05$; **$p < 0.01$; and ***$p < 0.001$.

of SphK1 siRNA induced a marked decrease in SphK1 protein expression in the resistant cancer cell lines compared with the control cells (Supplementary Figure E1; online only, available at www.exphem.org), while K562-SphK1 showed overexpression of SphK1, confirmed by Northern blot and Western blot analysis (Supplementary Figure E1B, C; online only, available at www.exphem.org) and induced ectopic levels very similar as those observed in IM/R selected cells. Likewise, SphK1 activity levels was also significantly decreased in K562 IM/R 0.6 μM treated with DMS to a similar extent as with SphK1 siRNA (Fig. 3C).

Concomitantly, downregulation of SphK1 expression and activity by DMS or siRNA significantly enhanced cell death in these reprogrammed cells, whereby >70% of the cells exposed to DMS showed IM-induced killing (Fig. 4A), suggesting activation of SphK1 has a dominant role in the mechanism of drug resistance. Likewise, knockdown of SphK1 also resulted in a significant induction of cell death in resistant cancer cells in response to IM, while overexpression of SphK1 in sensitive K562 cells prevented cell death in response to IM (Fig. 4C). To verify induction of apoptosis, we also employed an antibody specific for
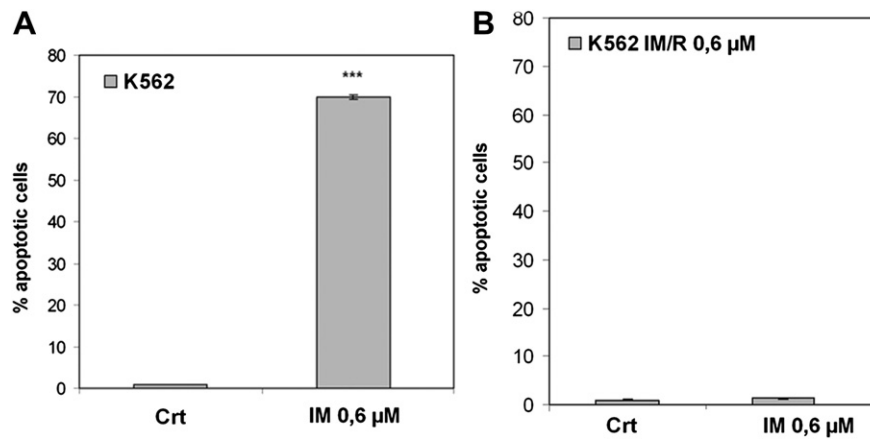
Figure 2. Induction of apoptosis in native (**A**), K562 cells control and treated with 0.6 μM IM for 72 hours (**B**) K562 IM/R 0.6 μM cells control and treated with 0.6 μM IM for 72 hours. K562 cells were prepared as in Figure 1, after which they were treated with the indicated concentration of 0.6 μM IM for 72 hours. Apoptosis induction was measured using an Annexin-V detection kit and the data are presented as percent of apoptotic cells. Bars represent the mean ± standard error of mean (SEM) of the results from three separate experiments. Significant differences between resistant cells and control cells are indicated by probability p values. *$p < 0.05$; **$p < 0.01$; and ***$p < 0.001$.

activated caspase-3, or an antibody that detects poly(ADP-ribose) polymerase cleavage. As shown in Figure 5, addition of DMS to K562-SphK1 or K562 IM/R 0.6–1 μM cells treated with IM activated both caspase-3 and poly(ADP-ribose) polymerase as well as in K562 IM/R 0.6–1 μM SphK1 siRNA treated with IM (Fig. 5A, B and Supplementary Figure E2A, B; online only, available at www.exphem.org). These data clearly reveal a functional role for SphK1 in regulating resistance to IM-induced apoptosis.
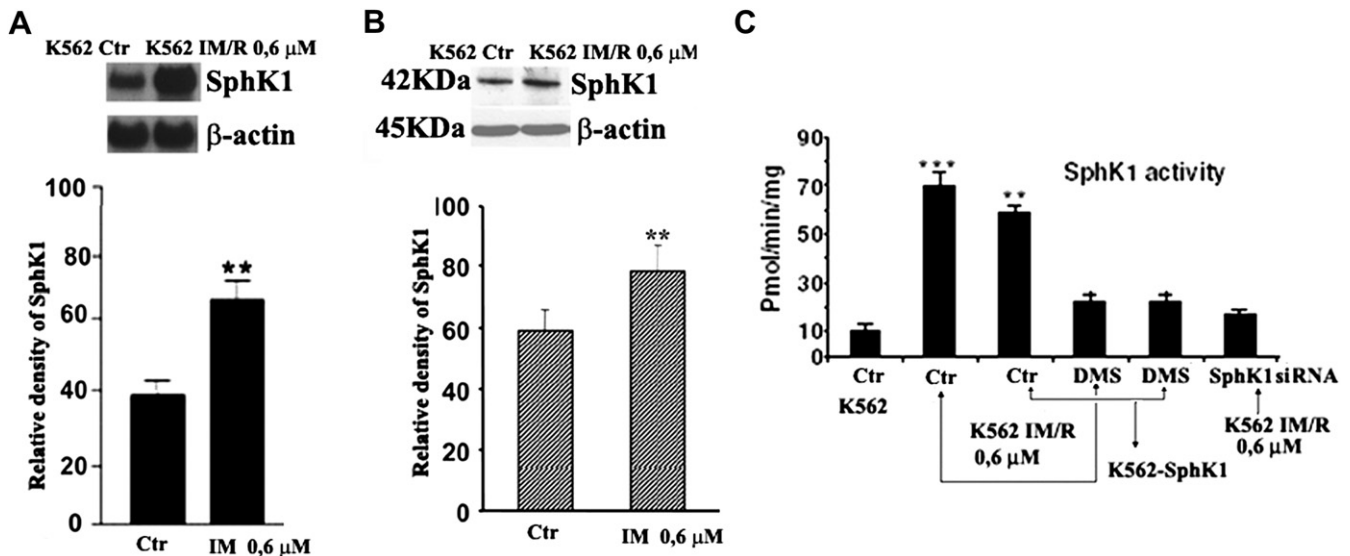

Figure 3. Expression levels of mRNA transcript, expression protein, and enzymatic activity levels of SphK1 in K562, K562 IM/R 0.6 μM, K562 IM/R 0.6 μM SphK1 siRNA, and K562-SphK1 cells. Northern blot and Western blot analysis were performed. β-actin was used as an internal loading control. (**A**) Total mRNAs were extracted from K562 and K562 IM/R 0.6 μM cells and analyzed by Northern blot. The membrane was hybridized with a ^{32}P-labeled probe for SphK1. Densitometric analysis of blots relative to SphK1. The bars represent mean ± standard error of mean of the results from three separate experiments. Significant differences between IM-resistant cells and control cells are indicated by probability p values. *$p < 0.05$; **$p < 0.01$; and ***$p < 0.001$. (**B**) Whole-cell lysates were prepared from K562 and K562 IM/R 0.6 μM cells and analyzed by Western blot using SphK1 specific antibodies. β-actin was used as a control for protein loading. The molecular weight (in KDa) of protein size standards is shown on the left-hand side. Densitometric analysis of blots relative to SphK1. Bars represent the mean ± standard error of mean of the results from three separate experiments. Significant differences between IM-resistant cells and control cells are indicated by probability p values. *$p < 0.05$; **$p < 0.01$; and ***$p < 0.001$. (**C**) Effect of DMS and SphK1-specific siRNA on SphK1 activity levels in K562 IM/R 0.6 μM, K562-SphK1 and in K562 IM/R 0.6 μM SphK1 siRNA cells. SphK1 activity levels determined by the in vitro SphK1 activity assay in K562 IM/R 0.6 μM cells treated with DMS (1 μM for 72 hours) and siRNA (for 48 hours) and in K562-SphK1 treated with DMS (1 μM for 72 hours). Bars represent the mean ± standard error of mean of the results from three separate experiments. Significant differences between resistant cells and control cells are indicated by probability p values. *$p < 0.05$; **$p < 0.01$; and ***$p < 0.001$.
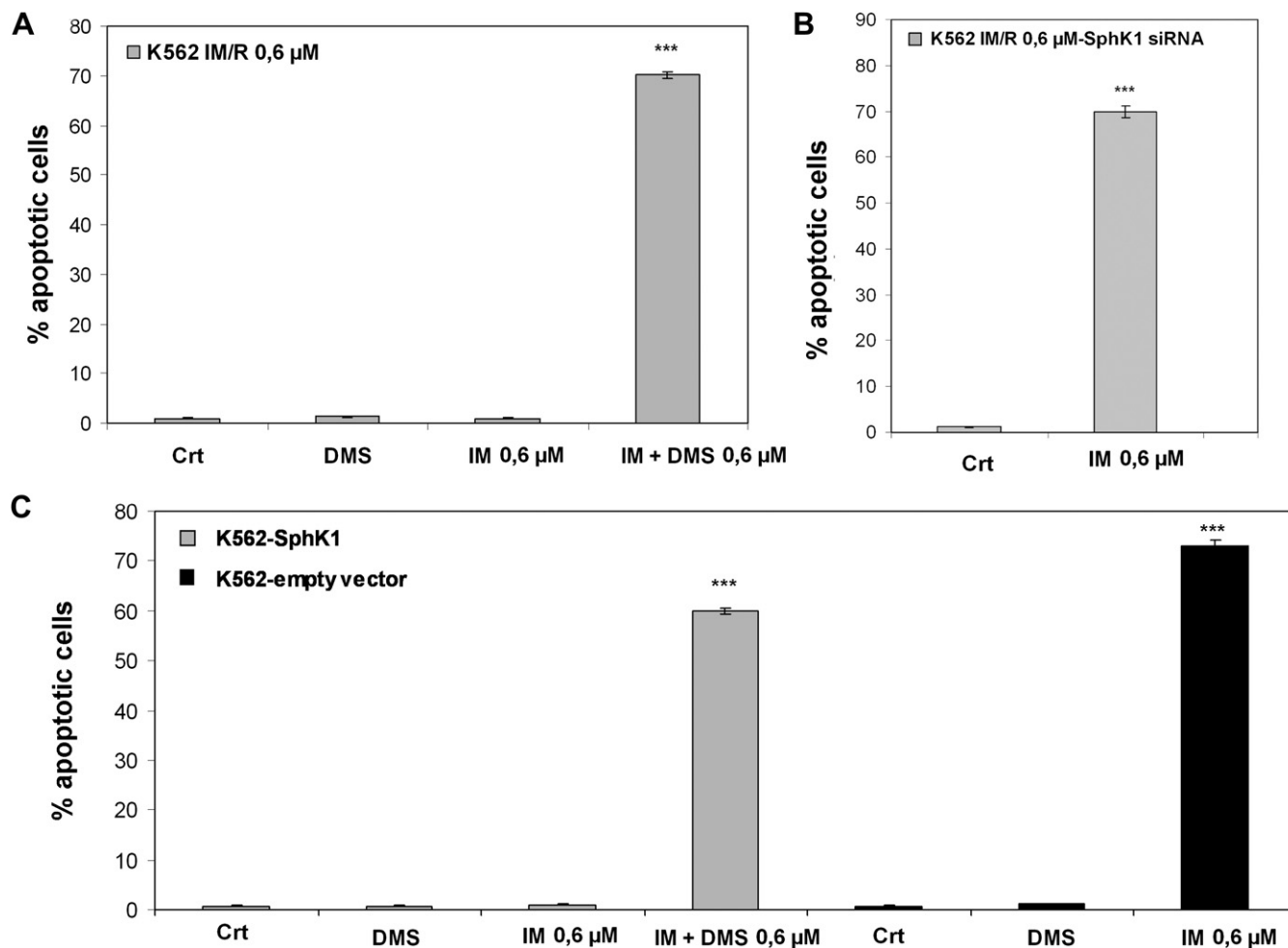
Figure 4. Induction of apoptosis in K562 IM/R 0.6 μM cells treated with DMS (1 μM for 72 hours) alone, 0.6 μM IM (72 hours) alone, and their combination for 72 hours. (**A**) K562 IM/R 0.6 μM cells control and treated with DMS (1 μM for 72 hours) alone, 0.6 μM IM (72 hours) alone, and in their combination for 72 hours. (**B**) K562 IM/R 0.6 μM cells transfected with a SphK1-specific siRNA and treated with 0.6 μM IM for 72 hours. (**C**) K562 cells transfected with SphK1 (K562-SphK1) or empty vector treated for 72 hours with DMS (1 μM) alone, 0.6 μM IM (72 hours) alone, or their combination for 72 hours. Bars represent the mean ± standard error of mean of the results from three separate experiments. Significant differences between resistant cells and control cells are indicated by probability p values. *$p < 0.05$; **$p < 0.01$; and ***$p < 0.001$.

Downregulation of c-Src and Erk1/2 does not influence apoptosis in IM-treated K562 IM/R

A recent study showed that elevated Src family kinase activity is sufficient to induce IM resistance through a mechanism that may involve phosphorylation of BCR-ABL [37]. Therefore, we measured the upregulation of c-Src and Erk1/2 in K562 IM/R 0.6–1 μM cells. Neither levels of Src or Erk1/2 were altered in K562 IM/R cells compared with sensitive K562 cells (Supplementary Figure E3A, B; online only, available at www.exphem.org). In addition, apoptosis in the K562 cells was not significantly induced by exposure to 4-amino-5-(4-chlorophenyl)-7-(t-butyl) pyrazolo[3,4-d]pyrimidine (10 μM) for 72 hours (a c-Src inhibitor) and PD98059 (50 μM) for 72 hours (an ERK selective inhibitor) (Supplementary Figure E4; online only, available at www.exphem.org). Likewise, knockdown of c-Src and Erk1/2, obtained with specific inhibitors and

siRNA, caused no significant induction of apoptosis in our resistant cancer cells (IM/R 0.6–1 μM) in response to IM (Supplementary Figure E4B, C, D, E; online only, available at www.exphem.org). Thus, these data reveal that c-Src and Erk1/2 proteins are not analogous to SphK1 in regulating resistance to IM in the K562 IM/R 0.6–1 μM reported in this study.

SphK1 mediates upregulation of BCR-ABL and activation of downstream signaling

Having established that SphK1 protected K562 IM/R cells from apoptosis, we next examined whether SphK1/S1P plays a functional role in the upregulation of BCR-ABL protein in IM/R selected K562 cells. Interestingly, forced expression of SphK1 in K562 cells (K562-SphK1) resulted in increased BCR-ABL protein levels, while partial inhibition of SphK1 expression using DMS or siRNA in K562
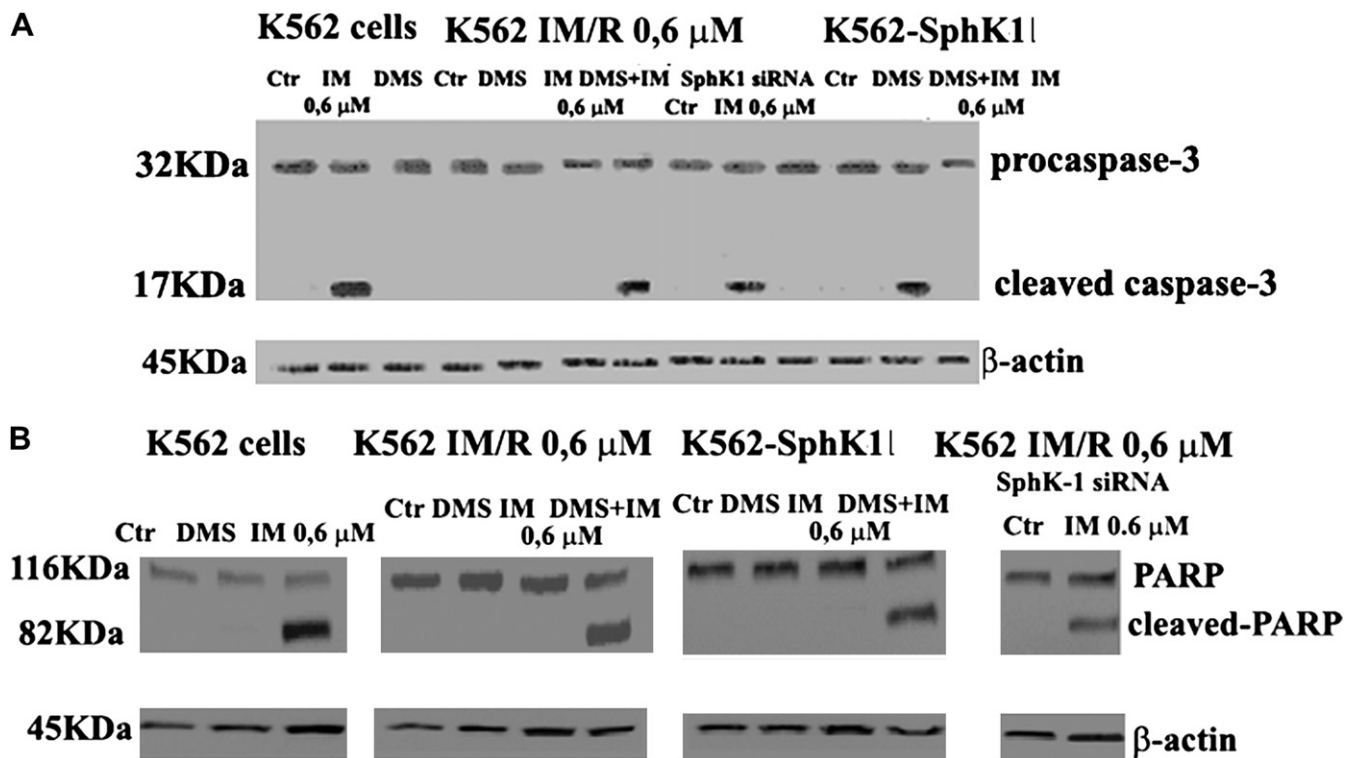
A

B

Figure 5. Activation of caspase-3 and poly(ADP-ribose) polymerase (PARP) in K562 cells, K562 IM/R 0.6 μM, K562-SphK1, and K562 IM/R 0.6 μM SphK1 siRNA. (**A**) K562 cells control and treated with DMS (1 μM for 72 hours) and 0.6 μM IM for 72 hours; K562 IM/R 0.6 μM and K562-SphK1 cells control and treated with DMS (1 μM for 72 hours) alone, 0.6 μM IM (72 hours) alone and their combination; K562 IM/R 0.6 μM cells transfected with a SphK1-specific siRNA and treated with 0.6 μM IM for 72 hours. Whole-cell lysates were prepared from all cell lines analyzed by Western blot using caspase-3 specific antibody. β-actin was used as a control for protein loading. The molecular weight (in KDa) of protein size standards is shown on the left-hand side. Blot is representative of three separate experiments. (**B**) K562 cells control and treated with DMS (1 μM for 72 hours) and 0.6 μM IM for 72; K562 IM/R 0.6 μM control and K562-SphK1 cells control and treated with DMS (1 μM for 72 hours) alone, 0.6 μM IM (72 hours) alone and their combination; K562 IM/R 0.6 μM cells transfected with a SphK1-specific siRNA and treated with 0.6 μM IM for 72. Whole-cell lysates were prepared from all cell lines analyzed by Western blot using PARP-specific antibody. β-actin was used as a control for protein loading. The molecular weight (in KDa) of protein size standards is shown on the left-hand side. Blot is representative of three separate experiments.

IM/R 0.6 μM resulted in decreased BCR-ABL protein levels (Fig. 6A, B). In contrast, SphK1 siRNA did not have any detectable effects on the mRNA levels of BCR-ABL measured by real-time PCR (data not shown), suggesting that SphK1 may affect downregulation of active BCR-ABL at the post-transcriptional level [12].

To further investigate whether increased SphK1 enzymatic activity resulted in activation of downstream signaling, we analyzed the tyrosine phosphorylation of Crk, a well-characterized substrate for SphK1 and SIP. Crk is an SH2 and SH3 domain-containing adaptor protein that binds to a proline-rich motif juxtaposed to ABL kinase domain. Crk binding to ABL kinase domain results in Crk phosphorylation on tyrosine-221 (which downmodulates Crk signaling) and on two recently discovered sites, tyrosine-239 and tyrosine-251, which stimulate downstream signaling (Birge, unpublished data). While no significant difference in the protein levels of Crk were detected, levels of tyrosine-221 phosphorylation of Crk was increased in all resistant cancer cell lines and SphK1 transfected cell lines when compared

to controls (Fig. 7A, B). Similarly, partial inhibition of SphK1 expression in K562 cells lines using DMS and siRNA resulted in a decreased tyrosine-221 phosphorylation of Crk with respect to controls (Fig. 7A, B). Interestingly, the levels of tyrosine-239 and -251 phosphorylation were also increased in K562-resistant and SphK1 transfected cells (Fig. 7A, B). In contrast, partial inhibition of SphK1 expression in resistant K562 cells lines by DMS and siRNA treatments decreased tyrosine-239 and -251 phosphorylation of Crk (Fig. 7A, B). These data suggest that SphK1 controls the levels of BCR-ABL in leukemia cells and this manifests activation of downstream signaling pathways.

Sphk1 expression is specifically regulated by the PI3K, AKT2, and mTOR pathways
Once we had established that IM resistance resulted in up-regulation of SphK1 expression and its enzymatic activity, we next examined the signaling molecules that modulate SphK1 expression and activation in K562 IM/R cells. Two promitogenic signaling pathways that have been
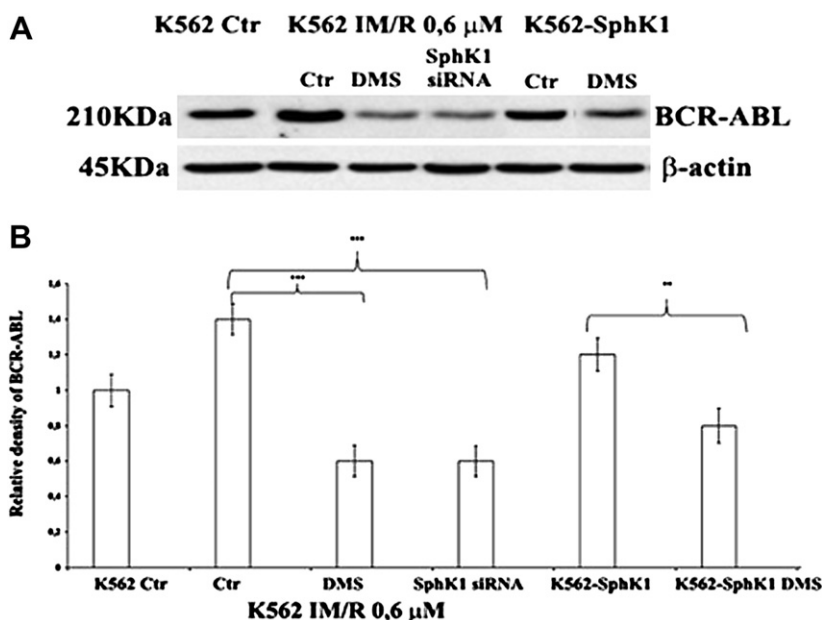
Figure 6. Effects of SphK1 inhibition on expression level of BCR-ABL protein in K562 IM/R 0.6 μM and K562-SphK1 cells. (**A**) Whole-cell lysates were prepared from K562 cells, K562 IM/R 0.6 μM, and K562-SphK1 cells (both cell lines treated with DMS 1 μM for 72 hours) and K562 IM/R 0.6 μM SphK1 siRNA for 48 hours. Western blot analysis was performed with an antibody specifically recognizing BCR-ABL protein. β-actin was used as an internal loading control. The molecular weight (in KDa) of protein size standards is shown on the left-hand side. Blot is representative of three separate experiments. (**B**) Densitometric analysis of blots relative to BCR-ABL. Bars represent the mean ± standard error of mean of the results from three separate experiments. Significant differences between IM-resistant cells and control cells are indicated by probability p values. *$p < 0.05$; **$p < 0.01$; and ***$p < 0.001$.

linked to activation of SphK1 signaling are the PI3K/AKT pathway [38] and the PKC pathway [39]. To determine if either of these pathways are involved in upregulation of SphK1 expression, we examined the levels of phospho-AKT and phospho-PKC levels in K562 IM/R $0.6-1$ μM. Phospho-AKT levels showed a increase in K562 IM/R $0.6-1$ μM, while the phospho-PKC levels did not change in resistant cells (Supplementary Figure E5A; online only, available at www.exphem.org). For this reason, we used pharmacological inhibitors that target the PI3K, AKT, and mTOR pathways. As indicated in Figure 8, when K562 IM/R cells were treated for 72 hours with either a PI3K inhibitor (100 nM wortmannin), an AKT inhibitor (5 μM SH-5), or a mTOR inhibitor (1 μM everolimus), the SphK1 protein levels decreased. In contrast, no significant change in SphK1 protein expression was observed in wild-type K562 cells pretreated with these inhibitors (Supplementary Figure E5B; online only, available at www.exphem.org). We next examined the effect of the isoform-specific AKT siRNAs on SphK1 mRNA levels. Reduction of AKT1 or AKT3 levels with siRNA did not have an effect on SphK1 mRNA levels (Fig. 8C, Supplementary Figure E6; online only, available at www.exphem.org). In contrast, knockdown of AKT2 significantly decreased SphK1 mRNA levels (Fig. 8C). We also determined if knocking down the AKT isoforms would have an effect on SphK1 protein expression levels and found

that AKT2 knockdown decreased the SphK1 expression protein levels (Fig. 8D). In contrast, suppressing AKT1 or AKT3 did not significantly alter the SphK1 mRNA protein levels (Fig. 8D) and enzymatic activity (Fig. 8E). The decrease that was noted in SphK1 activity was not affected by transfection with AKT1 or AKT3 siRNA (Fig. 8E). Knocking down AKT2, however, did reduce SphK1 activity levels to 75% in K562 IM/R 0.6 μM (Fig. 8E). These results indicate that AKT2 is predominantly involved in regulation of SphK1 mRNA protein levels in response to resistance in CML cells. In addition, knockdown of AKT2 decreased the BCR-ABL expression level in K562 IM/R $0.6-1$ μM, showing a role of SphK1 in regulation of BCR-ABL protein (Supplementary Figure E7; online only, available at www. exphem.org).

Discussion

In this study, we demonstrate a dominant role for Sphk1 in the acquisition of IM resistance in CML K562 cells. Specifically, we observe a strong correlation between IM resistance and SphK1 expression levels and activation status in K562 IM/R cells. These observations are based on several independent facts, which that include 1) resistant cancer cell lines exhibit elevated levels of SphK1 expression and enzymatic activity; 2) overexpression of SphK1 markedly reduces IM-induced cell growth arrest and apoptosis in nonresistant cancer cell
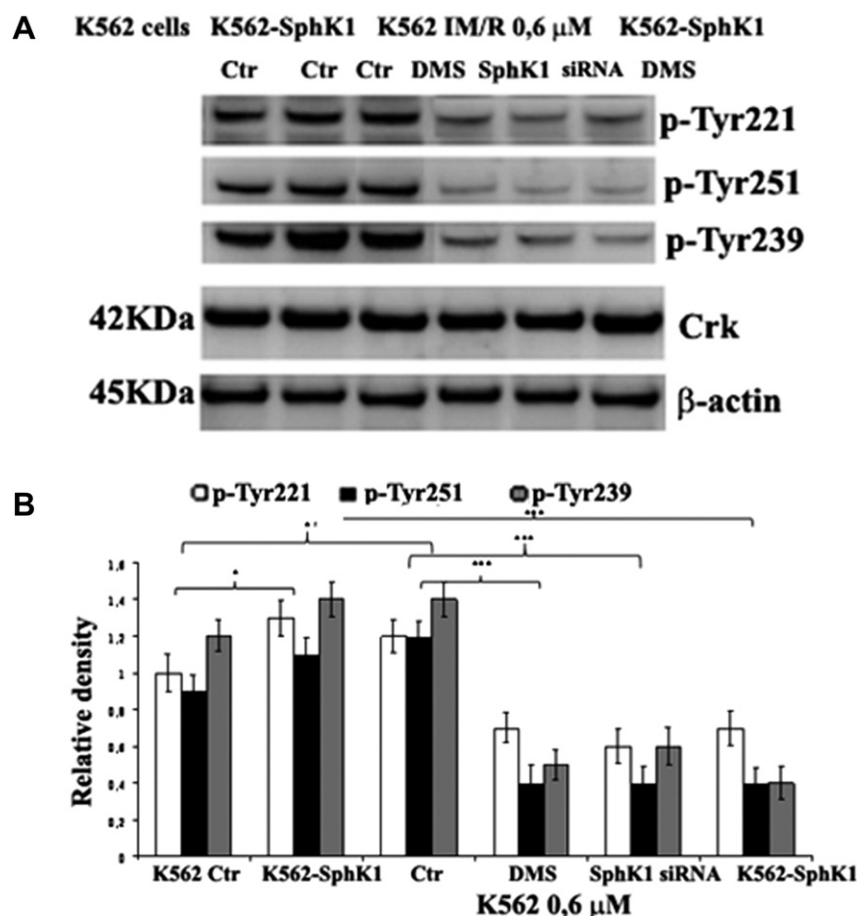
Figure 7. Effects of SphK1 upregulation on tyrosines phosphorylation of Crk in K562 IM/R 0.6 μM and K562-SphK1 cells. (**A**) Whole-cell lysates were prepared from K562 control, K562 IM/R 0.6 μM control, K562-SphK1 control, and specifically the latter two cell lines treated with DMS (1 μM for 72 hours) and K562 IM/R 0.6 μM SphK1 siRNA cells for 48 hours. Western blot analysis was performed with antibodies specifically recognizing p-Tyr251, p-Tyr239, p-Tyr221, and Crk protein. β-actin was used as an internal loading control. The molecular weight (in KDa) of protein size standards is shown on the left-hand side blot is representative of three separate experiments. (**B**) Densitometric analysis of blots relative to p-Tyr251, p-Tyr239, p-Tyr221 of Crk. Bars represent the mean ± standard error of mean of the results from three separate experiments. Significant differences between IM-resistant cells and control cells are indicated by probability *p* values. *$p < 0.05$; **$p < 0.01$; and ***$p < 0.001$.

lines; and 3) inhibition of SphK1 activity by chemical inhibition or by RNA interference restores the antiproliferative and proapoptotic effects and enhances sensitivity to IM. Mechanistically, we posit that a PI3K/AKT2 pathway plays a critical role for regulation of SphK1 expression because inhibition of either AKT2 or mTOR restores SphK1 levels, and concomitantly reverses chemoresistance toward IM. Our findings not only reveal a pivotal role of SphK1 in modulation of cellular sensitivity to IM, but also suggest that resistant status can be reprogrammed by manipulation of the SphK1 pathway. Moreover, our data suggest that combinational therapies that target SphK1 and TKI may delay drug resistance and have a clinical benefit in human cancers.

The mechanisms by which increased SphK1 expression participates in drug resistance are not fully resolved. Upregulated SphK1 would be expected to increased production of S1P, a metabolite that has been connected with multiple aspects of tumorigenesis, including regulation of cell survival, proliferation, differentiation, and cell migration [40]. Notably, there is also a growing body of evidence that SphK1 inhibition potentiates cancer cell response to radiotherapy- or chemotherapy-induced cell death [41,42] via a shift in S1P metabolism and increased ceramide production. Our findings, which demonstrate that SphK1 inhibition restores the susceptibility of the resistant cell lines to IM, are consistent with the idea that S1P induces cell survival mechanisms under the resistant status. Our results are also consistent with previous data showing a role for SphK1 in the regulation of drug-induced apoptosis via alteration of the ceramide/S1P balance and in the onset of chemotherapy resistance in leukemia [43] and in cells with multidrug-resistant phenotype [12,35,36,44].

While previous studies showed that mutations in the ABL kinase domain or activation of post-BCR-ABL−dependent
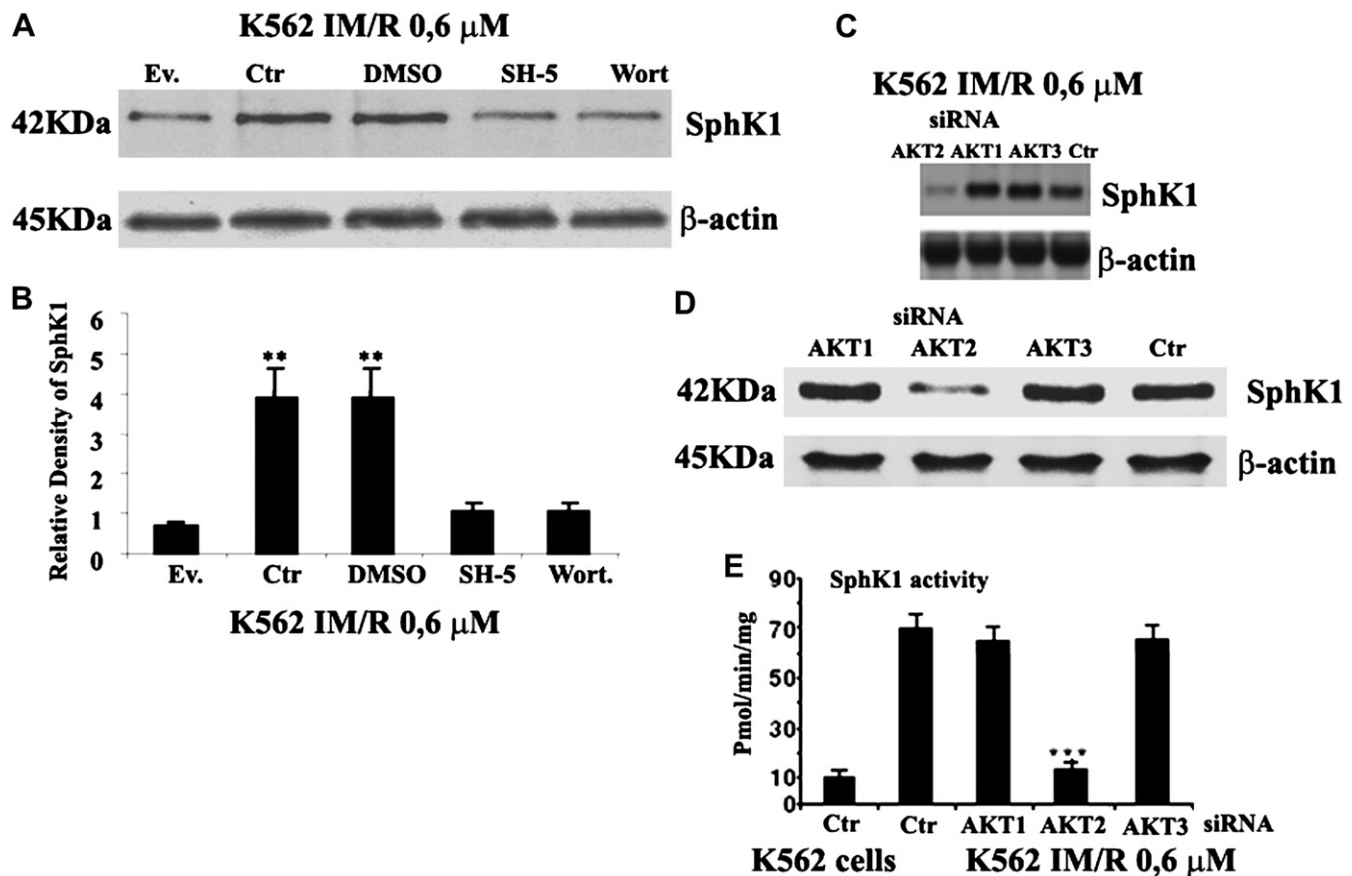
Figure 8. Effects of PI3K, AKT, and mTOR inhibitors and AKT1, AKT2, and AKT3 inhibition on SphK1 expression level in K562 IM/R 0.6 μM cells. (**A**) Whole-cell lysates were prepared from K562 IM/R 0.6 μM cells treated with a PI3K inhibitor (100 nM wortmannin), an AKT inhibitor (5 μM SH-5), an mTOR inhibitor (1 μM everolimus), or vehicle (dimethyl sulfoxide) for 72 hours. Western blot analysis was performed with an antibody specifically recognizing SphK1. β-actin was used as an internal loading control. The molecular weight (in KDa) of protein size standards is shown on the left-hand side. Blot is representative of three separate experiments. (**B**) Densitometric analysis of blots relative to SphK1. Bars represent the mean ± standard error of mean (SEM) of the results from three separate experiments. Significant differences between IM-resistant cells and control cells are indicated by probability p values. *$p < 0.05$; **$p < 0.01$; and ***$p < 0.001$. (**C**) Total mRNAs were extracted from K562 IM/R 0.6 μM cells transfected with AKT1, AKT2, and AKT3 siRNA for 48 hours. Northern Blot was performed with specific probe recognizing SphK1. β-actin was used as an internal loading control. (**D**) Whole-cell lysates were prepared from K562 IM/R 0.6 μM cells transfected with AKT1, AKT2, and AKT3 siRNA for 48 hours. Western blot analyses were performed with an antibody specifically recognizing SphK1. β-actin was used as an internal loading control. Molecular weight (in KDa) of protein size standards is shown on the left-hand side. Blot is representative of three separate experiments. (**E**) SphK1 activity levels determined by the in vitro SphK1 activity assay in K562 and K562 IM/R 0.6 μM cells transfected with AKT1, AKT2, and AKT3 siRNA for 48 hours. Bars represent the mean ± SEM of results from three separate experiments. Significant differences between resistant cells and control cells are indicated by probability p values. *$p < 0.05$; **$p < 0.01$; and ***$p < 0.001$.

pathways involving Erk1/2 and c-Src can infer drug resistance in CML [37], we did not observe mutations in ABL responsible in the K562 IM/R cells utilized in this study. Moreover, using either pharmacological inhibitors or siRNA-mediated knockdown of Erk1/2 or c-Src signaling, we did not observe restoration of IM sensitivity in the K562 IM/R cells. Although these data do not rule out that partial overlap exists in resistance pathways, our results suggest that SphK1 can play a dominant role in establishing a drug-resistant phenotype in K562 cells.

Increased SphK1 activity in IM/R selected cells, or forced SphK1 expression to comparably levels in nonselected cells, also concomitantly increases BCR-ABL expression, suggesting that SphK1 and SIP impinges on the stabilization of the BCR-ABL oncoprotein. Curiously, ectopic expression of

SphK1 had no effect on BCR-ABL mRNA, suggesting SphK1 affects the stability and turnover of BCR-ABL. The mechanisms for this interplay are not yet clear, although our data are consistent with the idea that SphK1 activity increases cellular SIP, which, in addition to suppressing apoptosis alluded to here, also impinges on tyrosine phosphorylation-dependent pathways. Indeed, previous studies by Endo and colleagues [45] showed that S1P potently stimulates phosphorylation of Crk on tyrosine-221 by inducing a complex amplification loop involving the S1P binding to its receptor, followed by receptor activation and subsequent activation of RTKs and c-Src family kinases. Ultimately, this pathway leads to stimulation of cytoskeletal assemblages and induces aggressive behavior in cells, such as increased cellular motility and invasion. In the Endo study [45], S1P-inducible cytoskeletal
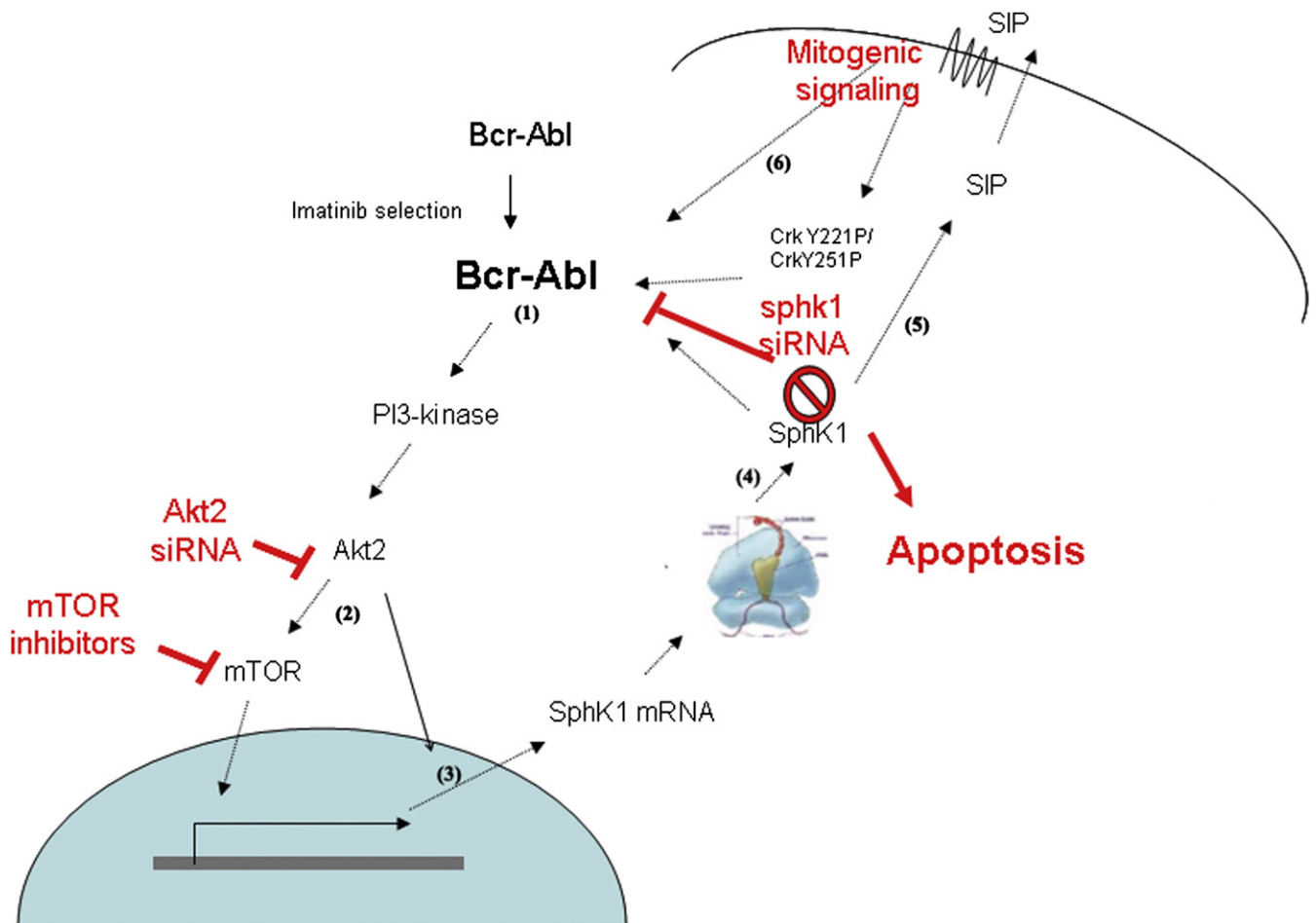
Figure 9. Model for SphK1 overexpression in K562 IM/R cells. Proposed mechanism of regulation of SphK1 overexpression mediated through the PI3K/AKT signaling pathway in K562 IM/R cells. (**1**) BCR-ABL is activated. (**2**) Downstream signaling molecules, AKT2 and mTOR. (**3**) Transcription of SphK1 is initiated, resulting in increased SphK1 mRNA levels. (**4**) SphK1 protein expression is elevated. (**5**) Activation of SphK1 results in increased production of S1P. (**6**) S1P signaling results in mitogenic signaling response.

reorganization was blocked by dominant-negative Crk proteins, suggesting tyrosine phosphorylation of Crk is important for SphK1 signaling. In this study, we found that Crk tyrosine 221 phosphorylation was dramatically increased in both IM/R K562 cells and was reversed by inhibiting SphK1 activity or downregulating SphK1 expression. In addition to S1P-inducible tyrosine-221 phosphorylation, tyrosine-221 on Crk can be phosphorylated directly by BCR-ABL. Therefore, whether Crk phosphorylation is directly mediated by an S1P-inducible pathway or indirectly mediated by SphK1-mediated upregulation of BCR-ABL (in K562 IM/R cells) is not clear.

Given the apparent centrality of SphK1 in IM/R K562 cells, another important question that arises is how SphK1 is elevated in the drug-resistant phenotype. Based on previous studies that suggested targeting the PI3K/AKT/mTOR pathway may have a direct apoptotic and antiproliferative effect on hematological malignancies [46,47], we used a battery of siRNA and pharmacological inhibitors to interrogate the relationship between SphK1 expression and activation of the PI3K/mTOR pathway. In particular,

PI3K pathway drives proliferation, apoptotic resistance, and cells expressing BCR-ABL show constitutive production of PIK3 and phosphorylation of AKT and its substrate [46]. Furthermore, the studies of other researchers have shown that two mTOR effectors, 4E-BP1 and S6K, are activated in a BCR-ABL kinase-dependent manner in BCR-ABL−expressing cell lines [48,49]. In mammalian cells, mTOR signaling depends on signal transmission through the PI3K/AKT pathway. Activated AKT phosphorylates TSC2, a component of tuberous sclerosis complexes 1 and 2, sensitive to nutrient status, and favors mTOR activity [50,51]. An important function of mTOR is the translation control via activation of ribosomal p70S6 kinase and suppression of 4E-BPs, resulting in enhanced translation of mRNAs encoding cell-cycle regulators and promotion of G_1–S cell-cycle transition [52].

In the present study, we found that silencing AKT2, but not ATK1 or ATK3, significantly reduced SphK1 mRNA and protein expression and enzymatic activity in IM/R K562 cells. This is consistent with previous reports that AKT2, but not

AKT3, is upstream of mTOR activation [53]. Based on our findings and another study [54], we propose a model of SphK1 overexpression and activation in K562 IM/R cells. In this model, overexpression of BCR-ABL activates PI3K and its downstream effectors, AKT2 and mTOR. Subsequently, SphK1 transcription levels are enhanced, resulting in increased SphK1 protein synthesis. The accumulated SphK1 enzyme phosphorylates sphingosine to elevate S1P levels, resulting in increased SphK1 enzymatic activity. S1P transmits mitogenic signals via binding to unidentified intracellular targets or via secretion extracellularly, where it can bind to S1P receptors on the cell surface of the same or neighboring cells. Aberrant activation of SphK1 could alter sphingolipid metabolism in favor of S1P, resulting in and/or hyperproliferative cellular responses, making SphK1 activation through AKT2, signaling an attractive target for resistance to TKI in leukemia (Fig. 9).

In conclusion, we have found a role for SphK1 in resistance to IM in human CML cancer cells and such drug-resistance phenotype correlated with increased level of BCR-ABL protein in K562 cells and subsequently increased kinase-inducible phosphorylation on the adaptor protein Crk. In addition, we demonstrate that the PI3K/AKT2/mTOR signaling pathway is involved in regulation of SphK1 and then signaling pathway can become an important therapeutic target. These data suggest that stabilization of a drug-resistant phenotype occurs through both activation of survival signals and activation of oncogene-directed signaling pathways.

Acknowledgments

Conflict of interest disclosure
No financial interest/relationships with financial interest relating to the topic of this article have been declared.

References
1. Rowley JD. Letter: a new consistent chromosomal abnormality in chronic myelogenous leukaemia identified by quinacrine fluorescence and Giemsa staining. Nature. 1973;243:290–293.
2. Kantarjian H, Dixon D, Keating MJ, et al. Characteristics of accelerated disease in chronic myelogenous leukemia. Cancer. 1988;61:1441–1446.
3. Goldman JM, Melo JV. Chronic myeloid leukemia advances in biology and new approaches to treatment. N Engl J Med. 2003;349:1451–1464.
4. Kantarjian H, Sawyers C, Hochhaus A, et al. International STI571 CML Study Group. Hematologic and cytogenetic responses to imatinib mesylate in chronic myelogenous leukemia. N Engl J Med. 2002;346:645–652.
5. Sawyers CL, Hochhaus A, Feldman E, et al. Imatinib induces hematologic and cytogenetic responses in patients with chronic myelogenous leukemia in myeloid blast crisis: results of a phase II study. Blood. 2002;99:3530–3539.
6. Schindler T, Bornmann W, Pellicena P, et al. Structural mechanism for STI-571 inhibition of abelson tyrosine kinase. Science. 2000;289:1938–1942.
7. Gambacorti-Passerini CB, Gunby RH, Piazza R, et al. Molecular mechanisms of resistance to imatinib in Philadelphia-chromosome-positive leukaemias. Lancet Oncol. 2003;4:75–85.
8. Krystal GW. Mechanisms of resistance to imatinib (STI571) and prospects for combination with conventional chemotherapeutic agents. Drug Resis Updates. 2001;4:16–21.
9. Hegedus T, Orfi L, Seprodi A, et al. Interaction of tyrosine kinase inhibitors with the human multidrug transporter proteins, MDR1 and MRP1. Biochim Biophys Acta. 2002;1587:318–325.
10. Deininger M. Resistance to imatinib: mechanisms and management. J Natl Compr Canc Netw. 2005;3:757–768.
11. Walz C, Sattler M. Novel targeted therapies to overcome imatinib mesylate resistance in chronic myeloid leukemia (CML). Crit Rev Oncol Hematol. 2006;57:145–164.
12. Baran Y, Salas A, Senkal CE, et al. Alterations of ceramide/sphingosine 1-phosphate rheostat involved in the regulation of resistance to imatinib-induced apoptosis in K562 human chronic myeloid leukemia cells. J Biol Chem. 2007;282:10922–10934.
13. Kharas MG, Janes MR, Scarfone VM, et al. Ablation of PI3K blocks BCR-ABL leukemogenesis in mice, and a dual PI3K/mTOR inhibitor prevents expansion of human BCR-ABL+ leukemia cells. J Clin Invest. 2008;118:3038–3050.
14. Um SH, Frigerio F, Thomas G, et al. Absence of S6K1 protects against age- and diet-induced obesity while enhancing insulin sensitivity. Nature. 2004;431:200–205.
15. Majumber PK, Febbo PG, Sellers WR, et al. mTOR inhibition reverses Akt-dependent prostate intraepithelial neoplasia through regulation of apoptotic and HIF-1-dependent pathways. Nat Med. 2004;10:594–601.
16. Ruggero D, Montanaro L, Ma L, et al. The translation factor eIF-4E promotes tumor formation and cooperates with c-Myc in lymphomagenesis. Nat Med. 2004;10:484–486.
17. Edsall LC, Van Brocklyn JR, Cuvillier O, et al. N N Dimethylsphingosine is a potent competitive inhibitor of sphingosine kinase but not of protein kinase C: modulation of cellular levels of sphingosine 1-phosphate and ceramide. Biochemistry. 1998;37:12892–12898.
18. Olivera A, Barlow KD, Spiegel S. Assaying sphingosine kinase activity. Methods Enzymol. 2000;311:215–223.
19. Xia P, Gamble JR, Wang L, et al. An oncogenic role of sphingosine kinase. Curr Biol. 2000;10:1527–1530.
20. Jendiroba DB, Klostergaard J, Keyhani A, et al. Effective cytotoxicity against human leukemias and chemotherapy-resistant leukemia cell lines by N-N-dimethylsphingosine. Leuk Res. 2002;26:301–310.
21. Maceyka M, Payne SG, Milstien S, Spiegel S. Sphingosine kinase, sphingosine-1-phosphate, and apoptosis. Biochim Biophys Acta. 2002;1585:193–201.
22. Le Scolan E, Pchejetski D, Banno Y, et al. Overexpression of sphingosine kinase 1 is an oncogenic event in erythroleukemic progression. Blood. 2005;106:1808–1816.
23. Van Brocklyn JR, Jackson CA, Pearl DK, et al. Sphingosine kinase-1 expression correlates with poor survival of patients with glioblastoma multiforme: roles of sphingosine kinase isoforms in growth of glioblastoma cell lines. J Neuropathol Exp Neurol. 2005;64:695–705.
24. Blakesly VA, Beitner-Johnson D, Van Brocklyn JR, et al. Sphingosine 1-phosphate stimulates tyrosine phosphorylation of Crk. J Biol Chem. 1997;272:16211–16215.
25. Birge RB, Kalodimos C, Inagaki F, Tanaka S. Crk and CrkL adaptor proteins: networks for physiological and pathological signalling. Cell Commun Signal. 2009;7:13.
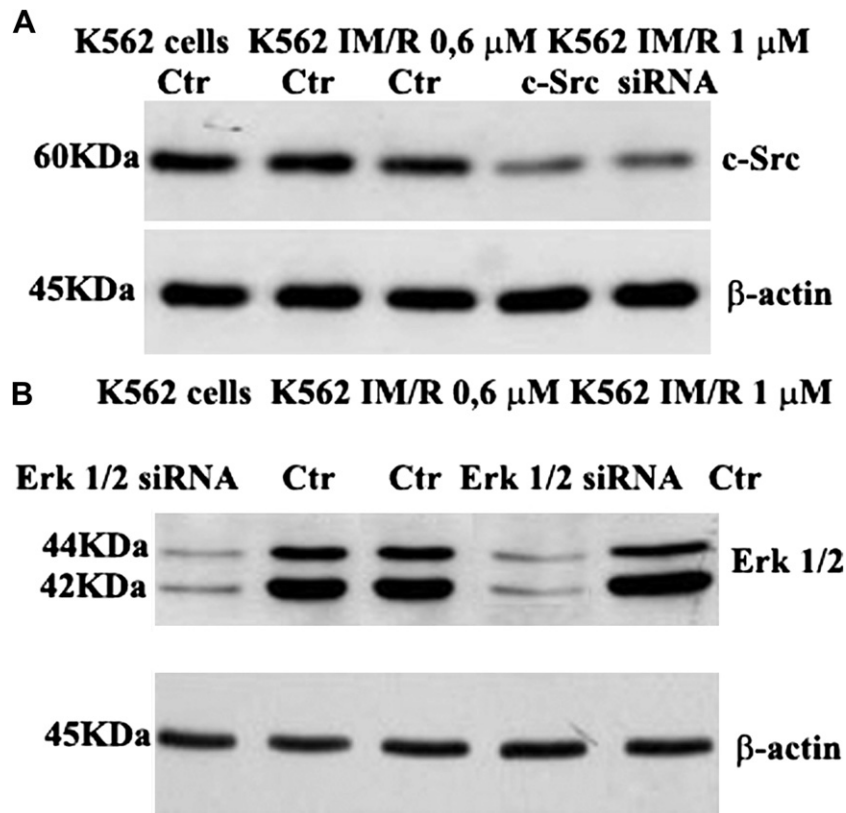
26. Mahon FX, Deininger MW, Schultheis B, et al. Selection and characterization of Bcr-Abl positive cell lines with differential sensitivity to the tyrosine kinase inhibitor STI571: diverse mechanisms of resistance. Blood. 2000;96:1070–1079.

27. Soverini S, Martinelli G, Amabile M, et al. Italian Cooperative Study Group on Chronic Myeloid Leukemia; European LeukemiaNet-6th Framework Program of the European Community. Denaturing-HPLC-based assay for detection of ABL mutations in chronic myeloid leukemia patients resistant to Imatinib. Clin Chem. 2004;50:1205–12013.

28. Sambrook J, Fritsch EF, Maniatis T. Molecular Cloning: A Laboratory Manual. Cold Spring Harbor, NY: Cold Spring Harbor Laboratory Press; 1989. p. 2.

29. Mensink E, van de Locht A, Schattenberg A, et al. Quantitation of minimal residual disease in Philadelphia chromosome positive chronic myeloid leukaemia patients using real-time quantitative RT-PCR. Br J Haematol. 1998;102:768–774.

30. Venkataraman K, Thangada S, Michaud J, et al. Extracellular export of sphingosine kinase-1a contributes to the vascular S1P gradient. Biochem J. 2006;397:461–471.

31. le Coutre P, Tassi E, Varella-Garcia M, et al. Induction of resistance to the Abelson inhibitor STI571 in human leukemic cells through gene amplification. Blood. 2000;95:1758–1766.

32. Kono K, Tanaka M, Ogita T, Hosoya T, Kohama T. F-12509A, a new sphingosine kinase inhibitor, produced by a discomycete. J Antibiotics (Tokyo). 2000;53:459–466.

33. Kohno M, Momoi M, Oo M, et al. Intracellular role for sphingosine kinase 1 in intestinal adenoma cell proliferation. Mol Cell Biol. 2006;26:7211–7223.

34. Bonhoure E, Pchejetski D, Aouali N, et al. Overcoming MDR-associated chemoresistance in HL-60 acute myeloid leukemia cells by targeting sphingosine kinase-1. Leukemia. 2006;20:95–102.

35. Bonhoure E, Lauret A, Barnes DJ, et al. Sphingosine kinase-1 is a downstream regulator of imatinib-induced apoptosis in chronic myeloid leukemia cells. Leukemia. 2008;22:971–979.

36. Ricci C, Onida F, Servida F, et al. In vitro anti-leukaemia activity of sphingosine kinase inhibitor. Br J Haematol. 2009;144:350–357.

37. Pene-Dumitrescu T, Smithgall TE. Expression of a Src family kinase in chronic myelogenous leukemia cells induces resistance to imatinib in a kinase-dependent manner. J Biol Chem. 2010;285:21446–21457.

38. Monick MM, Cameron K, Powers LS, et al. Sphingosine kinase mediates activation of extracellular signal-related kinase and Akt by respiratory syncytial virus. Am J Respir Cell Mol Biol. 2004; 30:844–852.

39. Johnson KR, Becker KP, Facchinetti MM, Hannun YA, Lina M, Obeid LM. PKC-dependent activation of sphingosine kinase 1 and translocation to the plasma membrane. Extracellular release of sphingosine-1-phosphate induced by phorbol 12-myristate 13-acetate (PMA). J Biol Chem. 2002;277:35257–35262.

40. Vadas M, Xia P, McCaughan G, Gamble J. The role of sphingosine kinase 1 in cancer: oncogene or non-oncogene addiction? Biochim Biophys Acta. 2008;1781:442–447.

41. Cuvillier O. Downregulating sphingosine kinase-1 for cancer therapy. Expert Opin Ther Targets. 2008;12:1009–1020.

42. Shida D, Takabe K, Kapitonov D, et al. Targeting SphK1 as a new strategy against cancer. Curr Drug Targets. 2008;9:662–673.

43. Sobue S, Iwasaki T, Sugisaki C, et al. Quantitative RT-PCR analysis of sphingolipid metabolic enzymes in acute leukemia and myelodysplastic syndromes. Leukemia. 2006;20:2042–2046.

44. Pchejetski D, Golzio M, Bonhoure E, et al. Sphingosine kinase-1 as a chemotherapy sensor in prostate adenocarcinoma cell and mouse models. Cancer Res. 2005;65:11667–11675.

45. Endo A, Nagashima K, Kurose H, et al. Sphingosine 1-phosphate induces membrane ruffling and increases motility of human umbilical vein endothelial cells via vascular endothelial growth factor receptor and CrkI. J Biol Chem. 2002;277:23747–23754.

46. Panwalkar A, Verstovsek S, Giles FJ. Mammalian target of rapamycin inhibition as therapy for hematologic malignancies. Cancer. 2004;100: 657–666.

47. Kharas MG, Fruman DA. ABL oncogenes and phosphoinositide 3-kinase: mechanism of activation and downstream effectors. Cancer Res. 2005;65:2047–2053.

48. Ly C, Arechiga AF, Walsh CM, Ong ST. Bcr-Abl kinase modulates the translation regulators ribosomal protein S6 and 4E-BP1 in chronic myelogenous leukemia cells via the mammalian target of rapamycin. Cancer Res. 2003;63:5716–5722.

49. Parmar S, Smith J, Sassano A, et al. Differential regulation of the p70 S6 kinase pathway by interferon alpha (IFN alpha) and imatinib mesylate (STI571) in chronic myelogenous leukemia cells. Blood. 2005;106: 2436–2443.

50. Manning BD, Tee AR, Logsdon MN, et al. Identification of the tuberous sclerosis complex-2 tumor suppressor gene product tuberin as a target of the phosphoinositide 3-kinase/akt pathway. Mol Cell. 2002;10:151–162.

51. Zhang Y, Gao X, Saucedo LJ, et al. Rheb is a direct target of the tuberous sclerosis tumour suppressor proteins. Nat Cell Biol. 2003;5:578–581.

52. Schmelzle T, Hall MN. TOR, a central controller of cell growth. Cell. 2000;103:253–262.

53. Hahn-Windgassen A, Nogueira A, Chen CC, et al. Akt activates the mammalian target of rapamycin by regulating cellular ATP level and AMPK activity. J Biol Chem. 2005;280:32081–32089.

54. Francy JM, Nag A, Conroy EJ, et al. Sphingosine kinase 1 expression is regulated by signaling through PI3K, AKT2, and mTOR in human coronary artery smooth muscle cells. Biochim Biophys Acta. 2007;269:253–265.

G. Marfe et al./ Experimental Hematology 2011;39:653–665
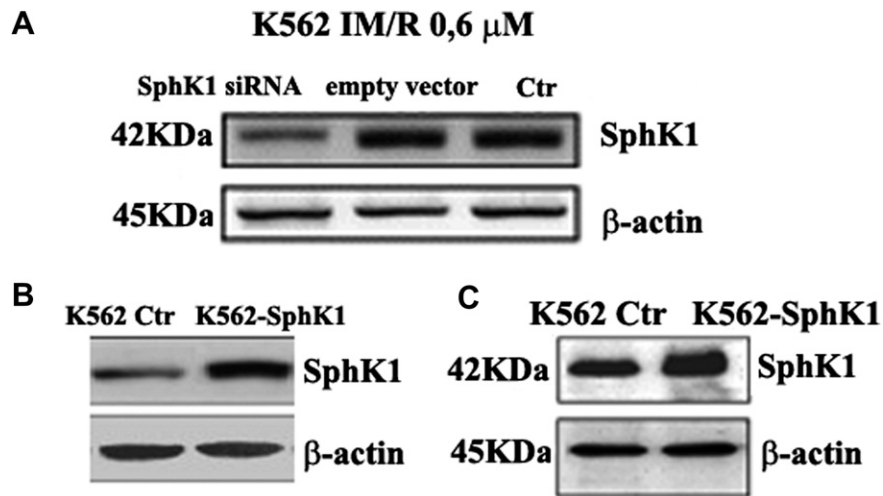
A **K562 IM/R 0,6 μM**

Supplementary Figure E1. SphK1 silencing by siRNA in K562 IM/R 0.6 μM and sensitive K562 cells transfected with SphK1 vector (K562-SphK1 cells). (**A**) Whole-cell lysates were prepared from K562 IM/R 0.6 μM and transfected with SphK1-specific siRNA or with an empty vector. Western blot analysis was performed using an antibody specifically recognizing SphK1 protein. β-actin was used as an internal loading control. Molecular weight (in KDa) of protein size standards is shown on the left-hand side. Blot is representative of three separate experiments. (**B**) Northern Blot analysis was performed in K562-SphK1 cells. β-actin was used as an internal loading control. (**C**) Western Blot analysis was performed in K562-SphK1 cells, using an antibody specifically recognizing SphK1 protein. β-actin was used as an internal loading control. Molecular weight (in KDa) of protein size standards is shown on the left-hand side. Blot is representative of three separate experiments.
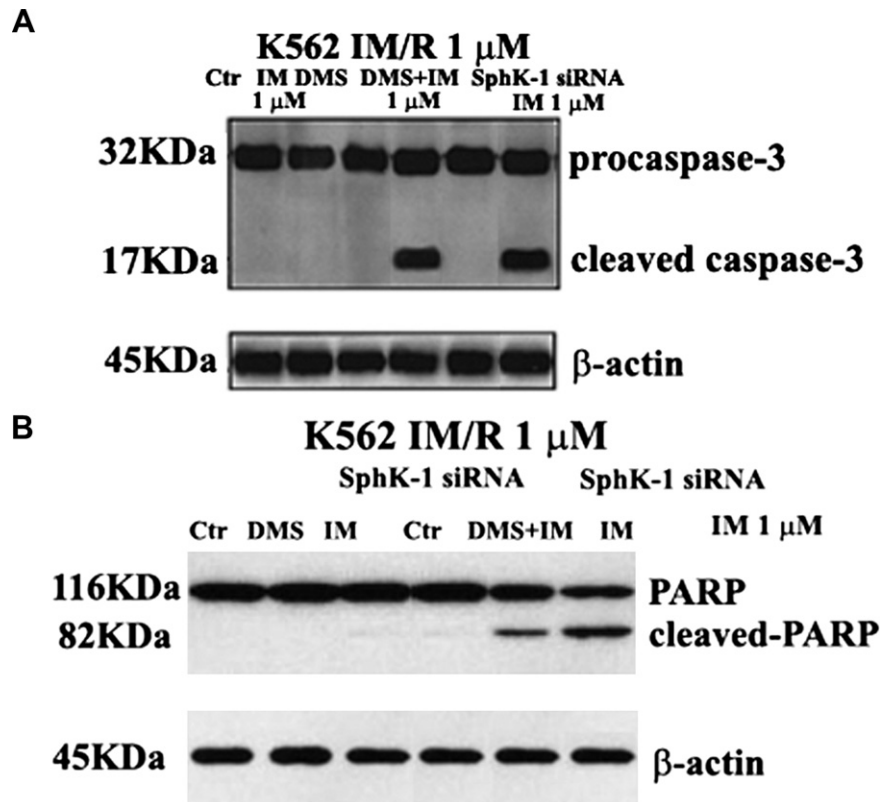
Supplementary Figure E2. Activation of caspase-3 and poly(ADP-ribose) polymerase (PARP) in K562 IM/R 1 µM and K562 IM/R 1 µM SphK1 siRNA cells. (**A**) K562 cells IM/R 1 µM treated with DMS (1 µM for 72 hours) alone, 1 µM IM (72 hours) alone, and their combination; K562 IM/R 1 µM cells transfected with a SphK1-specific siRNA and treated with 1 µM IM for 72 hours. Whole-cell lysates were prepared from all cell lines analyzed by Western blot using caspase-3−specific antibody. β-actin was used as a control for protein loading. Molecular weight (in KDa) of protein size standards is shown on the left-hand side. Blot is representative of three separate experiments. (**B**) K562 cells IM/R 1 µM treated with DMS (1 µM for 72 hours) alone, 1 µM IM (72 hours) alone, and their combination; K562 IM/R 1 µM cells transfected with a SphK1-specific siRNA and treated with 1 µM IM for 72 hours. Whole-cell lysates were prepared from all cell lines analyzed by Western blot using PARP-specific antibody. β-actin was used as a control for protein loading. Molecular weight (in KDa) of protein size standards is shown on the left-hand side. Blot is representative of three separate experiments.
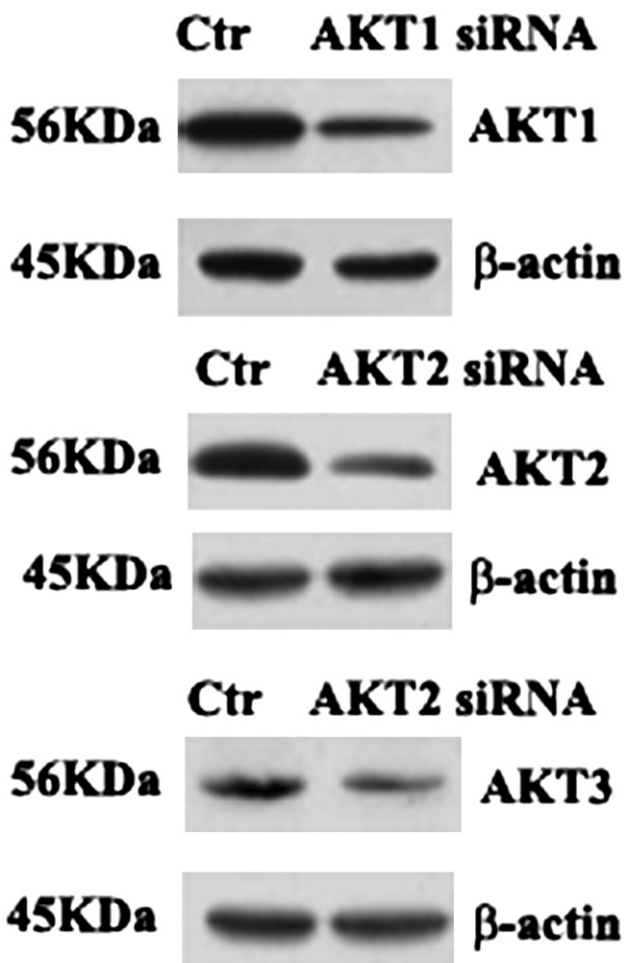
Supplementary Figure E3. Expression levels of c-Src and Erk1/2 in K562 and K562 IM/R 0.6−1 μM cells and K562 IM/R 0.6−1 μM cells silenced by Src and Erk1/2 siRNA. (**A**) Whole-cell lysates were prepared from K562 and K562 IM/R 0.6−1 μM cells and transfected with a c-Src−specific siRNA Western blot analysis was performed using an antibody specifically recognizing c-Src protein. β-actin was used as an internal loading control. Molecular weight (in KDa) of protein size standards is shown on the left-hand side. Blot is representative of three separate experiments. (**B**) Whole-cell lysates were prepared from K562 and K562 IM/R 0.6−1 μM cells and transfected with an Erk1/2-specific siRNA. Western blot analysis was performed using an antibody specifically recognizing Erk 1/2 protein. β-actin was used as an internal loading control. Molecular weight (in KDa) of protein size standards is shown on the left-hand side. Blot is representative of three separate experiments.
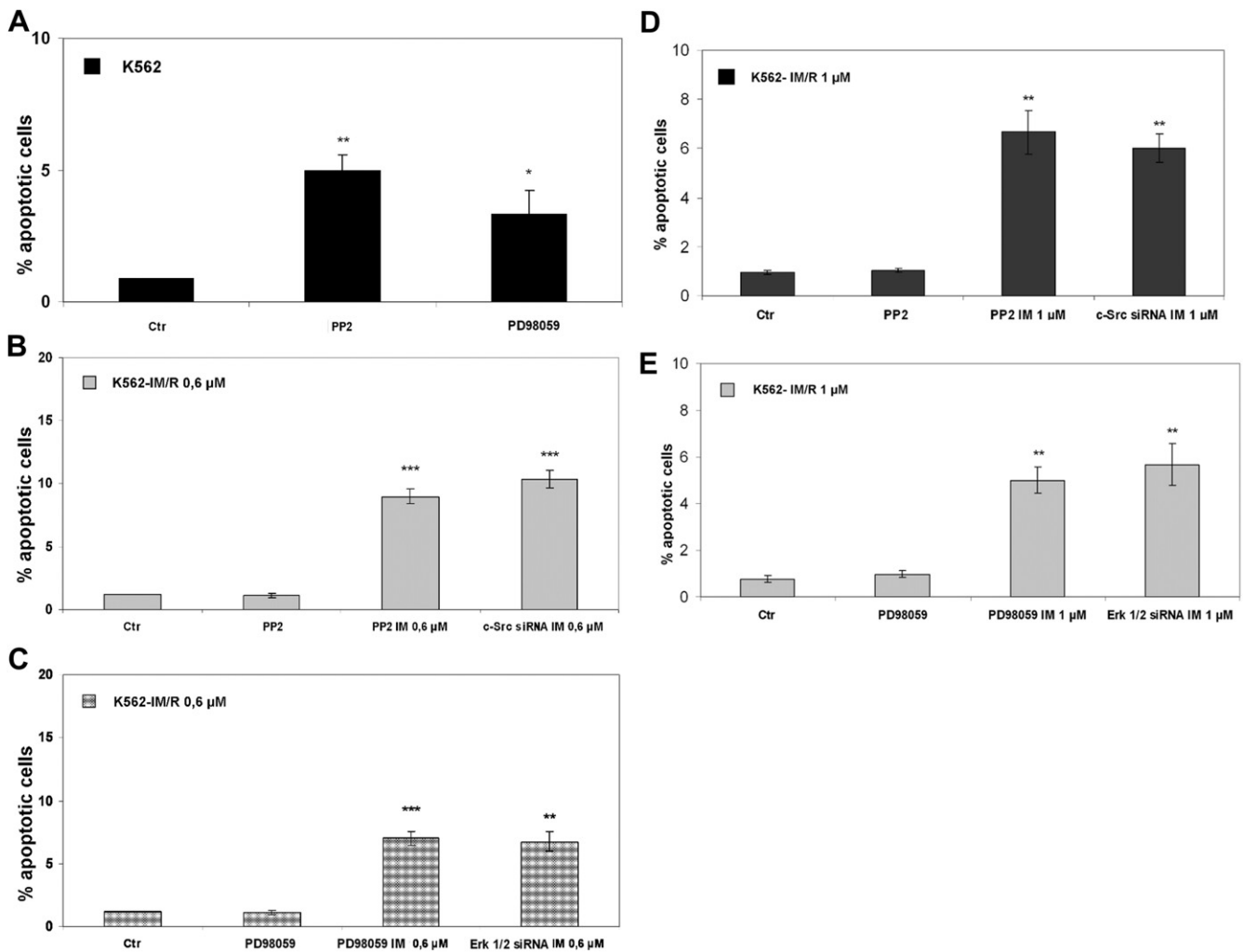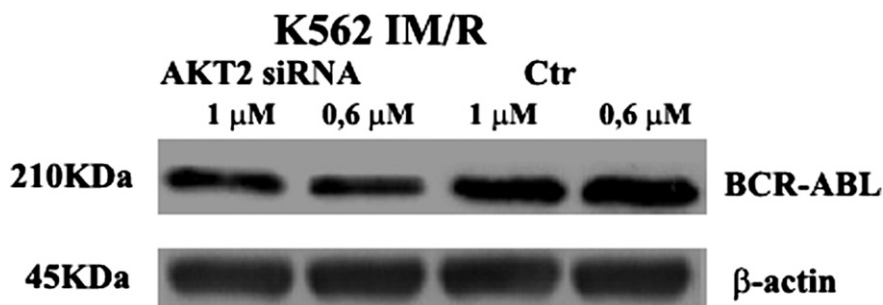
Supplementary Figure E4. Effects of c-Src and Erk1/2 inhibitors on apoptosis in K562 and K562 IM/R 0.6−1 μM cells and c-Src and Erk1/2 siRNA on apoptosis in K562 IM/R 0.6−1 μM cells. (**A**) K562 cells treated with 4-amino-5-(4-chlorophenyl)-7-(t-butyl)pyrazolo[3,4-d]pyrimidine (PP2; 10 μM) and PD98059 (50 μM) for 72 hours. (**B**) K562 IM/R 0.6 μM cells treated with PP2 (10 μM) alone for 72 hours, PP2 in combination with 0.6 μM IM for 72 hours, and K562 IM/R 0.6 μM cells transfected with a c-Src−specific siRNA and treated with 0.6 μM.IM for 72 hours. (**C**) K562 IM/R 0.6 μM cells treated with PD98059 (50 μM) for 72 hours alone, PD98059 in combination with 0.6 μM IM for 72 hours, K562 IM/R 0.6 μM cells transfected with a Erk1/2-specific siRNA and treated with 0.6 μM IM for 72 hours. (**D**) K562 IM/R 1 μM cells treated with PP2 (10 μM) alone for 72 hours, PP2 in combination with 1 μM IM for 72 hours, and K562 IM/R 1 μM cells transfected with a c-Src−specific siRNA and treated with 1 μM IM for 72 hours. (**E**) K562 IM/R 1 μM cells treated with PD98059 (50 μM) for 72 hours alone, PD98059 in combination with 1 μM IM for 72 hours, K562 IM/R 1 μM cells transfected with a Erk1/2-specific siRNA and treated with 1 μM IM for 72 hours. Bars represent mean ± standard error of mean of the results from three separate experiments. Significant differences between resistant cells and control cells are indicated by probability *p* values. *$p < 0.05$; **$p < 0.01$; and ***$p < 0.001$.

A

B
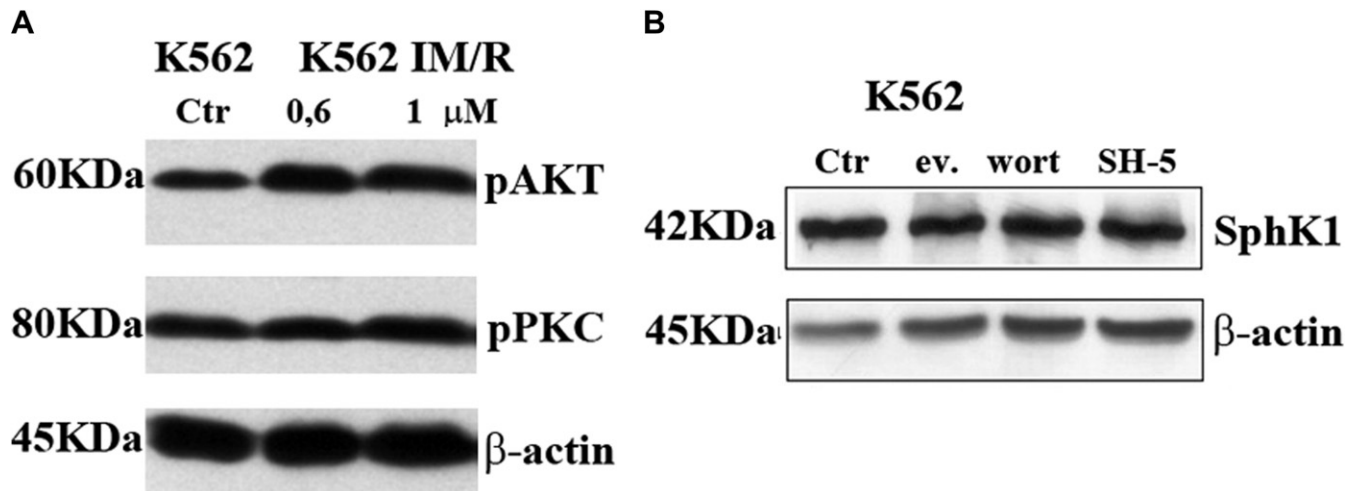
Supplementary Figure E5. Expression level of AKT and PKC phosphorylation in K562, and K562 IM/R 0.6−1 μM cells and effects of PI3K, AKT, and mTOR inhibitors on SphK1 expression in K562 cells. (**A**) Whole-cell lysates were prepared from K562 and K562 IM/R 0.6−1 μM cells. Western blot analysis was performed with antibodies specifically recognizing pAKT and pPKC. β-actin was used as an internal loading control. Molecular weight (in KDa) of protein size standards is shown on the left-hand side. Blot is representative of three separate experiments. (**B**) Whole-cell lysates were prepared from K562 cells treated with a PI3K inhibitor (100 nM wortmannin), an AKT inhibitor (5 μM SH-5), an mTOR inhibitor (1 μM everolimus), or vehicle (dimethyl sulfoxide) for 72 hours. Western blot analysis was performed with an antibody specifically recognizing SphK1. β-actin was used as an internal loading control. Molecular weight (in KDa) of protein size standards is shown on the left-hand side. Blot is representative of three separate experiments.

K562 IM/R 0,6 μM

Ctr   AKT1 siRNA

56KDa   AKT1

45KDa   β-actin

Ctr   AKT2 siRNA

56KDa   AKT2

45KDa   β-actin

Ctr   AKT2 siRNA

56KDa   AKT3

45KDa   β-actin

Supplementary Figure E6. AKT1, AKT2, and AKT3 silencing by siRNA in CML-resistant cell lines. Whole-cell lysates were prepared from K562 IM/R 0.6 μM cells and transfected with AKT1-, AKT2-, and AKT3-specific siRNA. Western blot analysis was performed with antibodies specifically recognizing AKT1, AKT2, and AKT3 protein. β-actin was used as an internal loading control. Molecular weight (in KDa) of protein size standards is shown on the left-hand side. Blot is representative of three separate experiments.

K562 IM/R

AKT2 siRNA   Ctr

1 μM   0,6 μM   1 μM   0,6 μM

210KDa   BCR-ABL

45KDa   β-actin

Supplementary Figure E7. Effects of AKT2 inhibition on expression level of BCR-ABL protein in K562 IM/R 0.6 and 1 μM. Whole-cell lysates were prepared from K562 IM/R 0.6 and 1 μM. Western blot analysis was performed with an antibody specifically recognizing BCR-ABL protein. β-actin was used as an internal loading control. Molecular weight (in KDa) of protein size standards is shown on the left-hand side. Blot is representative of three separate experiments.